14th Australasian Fluid Mechanics Conference
Adelaide University, Adelaide, Australia
10-14 December 2001

Spectral Element Based Dynamic Large Eddy Simulation of Turbulent Channel Flow

S. Schmidt and H. M. Blackburn

CSIRO Division of Building, Construction and Engineering
PO Box 56, Highett, Victoria, 3190 AUSTRALIA

Abstract

In this study the dynamic Smagorinsky model (DSM) has been incorporated into a spectral element method and applied in a large eddy simulation (LES) of a turbulent channel flow. The dynamic procedure estimates the parameter of the Smagorinsky model (SM), thereby allowing for an adaption of the mixing length to the local turbulent state during the simulation. As expected, strong fluctuations of the dynamic estimate arise which are due to the local nature of the model. To avoid any adverse influence to the convergence of the numerical scheme, most of these fluctuations are dampened out by averaging along the spanwise (homogeneous) direction and in time. Two different test filter kernels have been used in order to assess the quality and the robustness of the dynamic procedure and shed light on the dependency of the whole model on the test filter. The simulation results provide a good overall agreement with both experimental data and previous LES results, obtained with the fixed-constant Smagorinsky model.

Introduction

The successful application of LES to typical turbulent engineering flows depends to a large extent on the quality of the turbulence (i.e. subgrid-scale) model. Although much effort has been devoted to the development of improved subgrid-scale models, the majority of all LES still use a simple algebraic model (i.e. Smagorinsky model), because it has some striking advantages: it is computationally cheap, robust and often gives as good results as more complex models for a large variety of flows. However, it includes a model parameter which has to prescribed in advance and for complex flows, which are present in industrial applications, no unique value can be found. In addition, *ad hoc* modifications to the model parameter are required close to solid boundaries ("van Driest damping", vDd).

The dynamic procedure, first introduced by Germano et al. [2], bypasses theses problems since it is able to determine a local estimate of the mixing length, depending on the local state of the flow. This procedure, commonly known as the "dynamic model", has been successfully applied to many flows, mainly with finite-difference or finite-volume methods. Little is known of the application of the dynamic model in conjunction with spectral element methods [4, 6], although they are well-suited for LES, because of their highly desirable inherent numerical properties such as low dissipation and diffusion.

In previous work [1], we have described the application of the non-dynamic Smagorinsky-based spectral element LES to the turbulent channel flow with $Re_c = 13\,800$ ($Re_\tau = 640$). The present paper documents the implementation of the dynamic model within the spectral element framework and shows results of the successful application to the same flow. The channel flow was chosen for validation purposes, although the current formulation is not restricted to any type of geometry.

LES Methodology

The weakness of conventional (Reynolds-averaged Navier–Stokes, RANS) turbulence simulations, with universal models and a limited set of parameters, has promoted the use of LES. In order to reduce the influence of the turbulence model, the large scale structures, which carry most of the kinetic energy, are directly resolved by the grid. Since these large scales are dominated by geometrical constraints and boundary conditions, any initial orientation of turbulent structures gets lost during the energy cascade from large to smaller scales. Therefore the small-scale turbulence is expected to behave more isotropically, without any preferred orientation and should consequently be much easier to model than the whole spectrum of turbulence.

From a mathematical point of view, LES can be thought of as a convolution of the exact turbulent velocity field $\boldsymbol{u}$ with a filter kernel K that gives the resolved scale velocity field $\overline{\boldsymbol{u}}$,

$$\overline{\boldsymbol{u}}\,(\boldsymbol{r}) = \int K\left(\overline{\Delta}, |\boldsymbol{r}-\boldsymbol{r}'|\right)\ \boldsymbol{u}\,(\boldsymbol{r}')\ \mathrm{d}^3\boldsymbol{r}'. \qquad (1)$$

where $\overline{\Delta}$ is the filter length, which is usually be taken to be the grid size. The filtering operation is implicit in the formulation (i.e. not explicitly carried out). Under assumptions which are generally non-restrictive, filtering and differentiation commute, i.e. $\overline{\partial \boldsymbol{u}/\partial x} = \partial\overline{\boldsymbol{u}}/\partial x$. If LES is applied to distorted meshes, besides other numerical errors, an additional commutation error arises.

An equation for $\overline{\boldsymbol{u}}$ is obtained by convolving the Navier–Stokes equations with the same spatial filter function,

$$\partial_t\overline{\boldsymbol{u}} + \nabla\cdot\overline{\boldsymbol{u}\boldsymbol{u}} = -\nabla\overline{P} + \nu\nabla^2\overline{\boldsymbol{u}}\ , \qquad (2)$$

where $\overline{P} = \overline{p}/\rho$ for incompressible flows. As in conventional turbulence modelling, the nonlinear terms are have to be modelled, because the they cannot be expressed in terms of the known resolved components $\overline{\boldsymbol{u}}$. To overcome this problem, a subgrid-scale stress $\boldsymbol{\tau}$ is introduced (in a similar way to RANS modelling), such that $\boldsymbol{\tau} = \overline{\boldsymbol{u}\boldsymbol{u}} - \overline{\boldsymbol{u}}\,\overline{\boldsymbol{u}}$. The momentum equation then becomes

$$\partial_t\overline{\boldsymbol{u}} + \nabla\cdot\overline{\boldsymbol{u}}\,\overline{\boldsymbol{u}} = -\nabla\overline{P} + \nu\nabla^2\overline{\boldsymbol{u}} - \nabla\cdot\boldsymbol{\tau}. \qquad (3)$$

The turbulence modelling task is to estimate the subgrid-scale stress $\boldsymbol{\tau}$ from the resolved velocity field $\overline{\boldsymbol{u}}$.

Dynamic Subgrid-Scale Model

In LES, all length-scales of turbulence down to a cut-off wavenumber k_c are explicitly resolved, while the influence of the smallest scales down to the Kolmogorov (dissipation) length $\eta = (\nu^3/\varepsilon)^{1/4}$, are simulated by a

subgrid-scale model. By assumption, the maximum resolved wavenumber resides within the inertial subrange, where the kinetic energy scales with $k^{-3/5}$. In this region, turbulent kinetic energy is basically transported from large to small scales without any other effects like turbulent production or dissipation. At the cut-off wavenumber, the smallest resolved scales behave like the largest unresolved (subgrid-) scales of motion and consequently, their mixing-length should be similar. Therefore they should be able to be described with the same model with one model parameter. Applying a test filter at a lower cut-off wavenumber k_f enables us to resolve the turbulence on both sides of this border. The assumption, that the behaviour at k_f and k_c are comparable, is the basis of all dynamic procedures.

Test Filters

The first task in constructing the dynamic procedure is to define and apply a test-filter to equation (3). For comparison, we used two different explicit test filters, to investigate the influence of the filter function to the dynamic procedure and the flow prediction. Both filters only differ in the (x, y) plane, while the same spectral (Boyd-Vandeven [7]) Fourier filter is employed in the spanwise direction (z).

The first type of filter employs a spectral-projection technique. Filtering is done via elementwise projection of data from the space of Lagrange polynomials based on the Gauss–Lobatto (GL) points for the resolved mesh (here, order $N_p=8$) to a set order $N_p/2$, i.e. to a coarser GL mesh. The second discrete filter is a top-hat filter operating in physical space. This type of filter is typically used in finite-volume methods and is defined as (for 1-D)

$$\overline{\phi_i} = \frac{1}{6}\left(\phi_{i-1} + 4\,\phi_i + \phi_{i+1}\right),, \tag{4}$$

where $i-1$, i, and $i+1$ represent successive collocation points of the GL mesh. On a uniform mesh, the equivalent kernel is a box in physical space, having twice the length of the grid filter $\widetilde{\overline{\Delta}} = 2\,\overline{\Delta}$. This filter is applied elementwise without exchange of information at element boundaries. Figure 1 shows how both filters work on an initial field (1a). The spectral-projection filter (1b) retains some additional details of the flow compared to the top-hat filter (1c).

Dynamic Procedure

Applying a second filter with an associated size of $\widetilde{\overline{\Delta}}$ to the filtered Navier–Stokes equations (3) leads to a similar stress tensor on the test-filter level $\boldsymbol{T}$

$$\partial_t\widetilde{\overline{\boldsymbol{u}}} + \nabla\cdot\widetilde{\overline{\boldsymbol{u}}}\,\widetilde{\overline{\boldsymbol{u}}} = -\nabla\widetilde{\overline{P}} + \nu\nabla^2\widetilde{\overline{\boldsymbol{u}}} - \nabla\cdot\boldsymbol{T} \tag{5}$$

$$\text{with}\quad \boldsymbol{T} = \widetilde{\overline{\boldsymbol{u}}\,\overline{\boldsymbol{u}}} - \widetilde{\overline{\boldsymbol{u}}}\,\widetilde{\overline{\boldsymbol{u}}}\,. \tag{6}$$

Assuming similar physics underly both stresses $\boldsymbol{\tau}$ and $\boldsymbol{T}$, they can be modelled with the exactly the same model. Filtering of $\boldsymbol{\tau}$ gives $\widetilde{\boldsymbol{\tau}} = \widetilde{\overline{\boldsymbol{u}}\,\overline{\boldsymbol{u}}} - \widetilde{\overline{\boldsymbol{u}}}\,\widetilde{\overline{\boldsymbol{u}}}$ in which the first term on the r.h.s. matches the one in equation (6) and can therefore be eliminated, leading to the relation known as "Germano's Identity"

$$\boldsymbol{\mathcal{L}} = \boldsymbol{T} - \widetilde{\boldsymbol{\tau}} = \widetilde{\overline{\boldsymbol{u}}\,\overline{\boldsymbol{u}}} - \widetilde{\overline{\boldsymbol{u}}}\,\widetilde{\overline{\boldsymbol{u}}}\,, \tag{7}$$

which can be used with any stand-alone subgrid-scale model—all terms, except model parameter can be evaluated. For simplicity, we employ the Smagorinsky model $\boldsymbol{\tau} = -2\,\nu_t\,\overline{\boldsymbol{S}}$ with $\nu_t = (C_s\overline{\Delta})^2\,|\overline{\boldsymbol{S}}|$ and $|\overline{\boldsymbol{S}}| = \mathrm{tr}(2\,\overline{\boldsymbol{S}}^2)^{1/2}$.

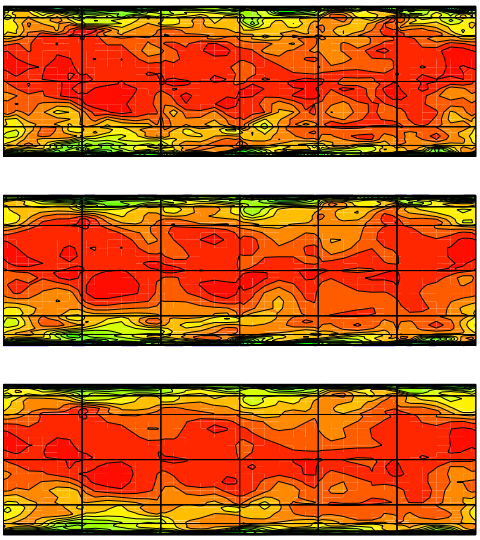

Figure 1: Test filters applied to initial field (a): spectral-projection filter (b) and top-hat filter (c).

The derivation of the dynamic procedure for estimation of the model parameter follows Lilly [8], which is numerically more stable than the original formulation [2]. Modelling of $\boldsymbol{\tau}$ and $\boldsymbol{T}$ gives

$$\boldsymbol{\tau} = -2\,(C_s\,\overline{\Delta})^2\,|\overline{\boldsymbol{S}}|\,\overline{\boldsymbol{S}}\,,\quad \boldsymbol{T} = -2\,(C_s\,\widetilde{\overline{\Delta}})^2\,|\widetilde{\overline{\boldsymbol{S}}}|\,\widetilde{\overline{\boldsymbol{S}}} \tag{8}$$

and applied to equation (7) this results in the quantity

$$\boldsymbol{\mathcal{L}} = -2\,(C_s\,\overline{\Delta})^2\boldsymbol{M} \tag{9}$$

with

$$\boldsymbol{M} = \left(\widetilde{\overline{\Delta}}/\overline{\Delta}\right)^2\,|\widetilde{\overline{\boldsymbol{S}}}|\,\widetilde{\overline{\boldsymbol{S}}} - |\widetilde{\overline{\boldsymbol{S}}}|\,\widetilde{\overline{\boldsymbol{S}}}\,,\quad \widetilde{\overline{\Delta}}/\overline{\Delta} = 2\,. \tag{10}$$

In order to obtain *one* dynamic estimate, the tensor equation (9) is reduced by double contraction, leading to

$$\boldsymbol{\mathcal{L}} : \boldsymbol{M} = -2\,(C_s\,\overline{\Delta})^2\boldsymbol{M}{:}\boldsymbol{M}\,, \tag{11}$$

from which the dynamic estimate can be derived

$$\left(C_s(x,y,z,t)\,\overline{\Delta}\right)^2 = -\frac{1}{2}\,\frac{\langle\boldsymbol{\mathcal{L}}{:}\boldsymbol{M}\rangle_z}{\langle\boldsymbol{M}{:}\boldsymbol{M}\rangle_z}\,. \tag{12}$$

This procedure evaluates a local and time-dependent value of C_s and is updated every time step. Note that the product $(C_s\,\overline{\Delta})$ is treated as a mixing length L_{Mix}, without explicitly specifying the length scale on the grid level $\overline{\Delta}$.

Stability problems usually force the use of spatial averaging along homogeneous directions (x, z) to limit the fluctuations of the model parameter. However, in the channel simulations we have only applied a spanwise averaging (as indicated by the z subscript in equation 12), to keep the implementation as general as possible. Note that the averaging is applied separately to the numerator and denominator of equation (12) before constructing the dynamic estimate. Additional time-averaging, using a running average

$$L_{\mathrm{Mix}}^{2\,(n)} = \varepsilon\,L_{\mathrm{Mix}}^2 + (1-\varepsilon)\,L_{\mathrm{Mix}}^{2\,(n-1)} \tag{13}$$

with ε in the range of $\varepsilon = 0.01 - 0.10$ reduces transient fluctuations and enables us to assess the quality of the model parameter after it has statistically converged. Further, clipping of the effective viscosity $\nu_T = \nu_t + \nu$ to eliminate negative values prevents large negative values of the eddy viscosity contaminating the solution, which could lead to convergence problems.

Numerical Method

The spatial discretisation employs a spectral element–Fourier formulation, which allows arbitrary geometry in the (x, y) plane, but requires periodicity in the z (out-of-plane) direction. The basis of the method as applied to the direct numerical simulation of the incompressible Navier–Stokes equations has been described by Karniadakis & Henderson [4]. The nonlinear terms of (3) have been implemented in a skew-symmetric form, i.e. $(\overline{\boldsymbol{u}} \cdot \nabla\overline{\boldsymbol{u}} + \nabla\overline{\boldsymbol{u}}\,\overline{\boldsymbol{u}})/2$, as this has been found to reduce aliasing errors [10]. These aliasing effects contaminate the resolved spectrum and usually lead to higher values of velocity fluctuations.

The method described in [4] requires modification in order to deal with the $\nabla\cdot\boldsymbol{\tau}$ terms in (3). The approach taken here follows that outlined in [1, 5], where the sum of the molecular and turbulent eddy viscosities $\nu_T = \nu_t + \nu$ is decomposed into a spatially-constant component ν_{ref} and a spatially-varying component $(\nu_T - \nu_{\text{ref}})$. The value of ν_{ref} is chosen to be approximately equal to the maximum value of ν_T. This value is not known *a priori*, but ν_{ref} can be adjusted during the computation without any adverse effects. When solving (3), the term $\nabla\cdot(\nu_T - \nu_{\text{ref}})\left[\nabla\overline{\boldsymbol{u}} + (\nabla\overline{\boldsymbol{u}})^t\right]$ is treated explicitly, while the term $\nu_{\text{ref}}\nabla^2\overline{\boldsymbol{u}}$, is treated implicitly, thus enhancing the overall numerical stability of the scheme.

As a result of the Fourier decomposition, implementation of the time integration as a parallel algorithm is straightforward, with inter-process communication required only during formulation of the nonlinear terms in (3). The message-passing kernel MPI has been used for this operation, and the computations reported here were carried out using 8 processors. In order to drive the flow in the streamwise (x) direction, a body force per unit mass of magnitude $2\tau_w/\rho$ was applied in the appropriate term in the filtered N–S equation.

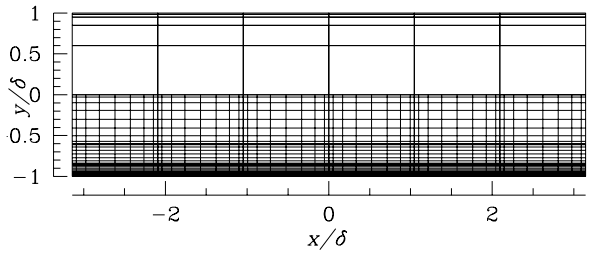

Figure 2: Two-dimensional section of 60-element mesh. The upper half of the mesh shows spectral element boundaries, the lower half shows the element nodes for 8×8 tensor-product shape functions.

Mesh parameters

For comparison with previous non-dynamic LES calculations, the same mesh as in [1] was used. The domain is spatially periodic in the streamwise and spanwise direction. The domain size was set to $L_y = 2\delta$ in the wall normal direction, $L_x = 2\pi\delta$ in the streamwise direction and $L_z = \pi\delta$ in the spanwise direction. The mesh consists of 60 elements (see figure 2), each discretized by 8×8 tensor-product shape functions leading to mesh sizes of $\Delta x^+ \simeq 50$–100, $\Delta z^+ \simeq 15$–40 while the first mesh point away from the walls was located at $y^+ < 1$. Using 64 planes of data in the z direction, the mesh has a total of 311 040 nodes.

Results

In figure 3, the mean velocity profiles are displayed in wall units: $u^+ = u/u_\tau$, $y^+ = y\,u_\tau/\nu$. For comparison purposes the experimental results of Hussain & Reynolds [3] at $Re_c = 13\,800$, $(Re_\tau = 640)$ and LDA measurements by Wei & Willmarth [9] at slightly higher $Re_c = 14\,900$ $(Re_\tau = 708)$ are shown, along with a 'Law of the Wall' plot which uses $u^+ = 2.5\ln y^+ + 5.0$ in the logarithmic region.

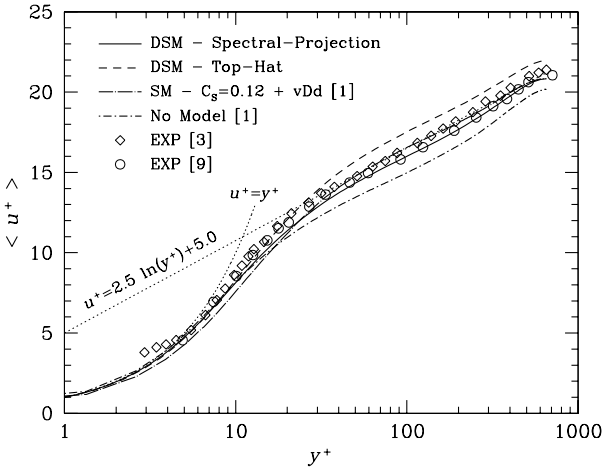

Figure 3: Mean velocity profiles.

The results obtained with the dynamic model using the two types of test filter are quite distinct. The spectral-projection filter achieves good agreement with the experimental values [3, 9] and the "best-fit" Smagorinsky model with $C_S = 0.12$, whereas the top-hat filter overshoots the data by a constant value in the logarithmic region $(y^+ > 30)$. Apparently, the choice of the test filter has an impact on the results. It should be emphasized that in order to get reasonable results from the non-dynamic Smagorinsky model (shown as SM in figure 3), the constant C_S has to be known in advance, and in addition, *ad hoc* van Driest damping must be incorporated near the walls. As expected, LES with no model contribution fails to reproduce the correct velocity distribution in the logarithmic region of the channel, confirming the importance of setting the model parameter correctly.

In figure 4, the profiles of the rms-values of the velocity fluctuations are shown with experimental data [3, 9] and previous LES results [1] for comparison. All computed streamwise fluctuations somewhat exceed the experimental levels, which display marked variation between measurement sets. The dynamic model with the spectral-projection filter gives similar results to the Smagorinsky model, besides predicting the stress peak closer to the wall (in agreement with experiment). The top-hat filter overestimates the streamwise fluctuations, while agreeing reasonably well for other values. The LES without any model clearly fails to correctly capture the anisotropy of the velocity fluctuations, as it produces the largest wall normal and spanwise fluctuations. As shown in

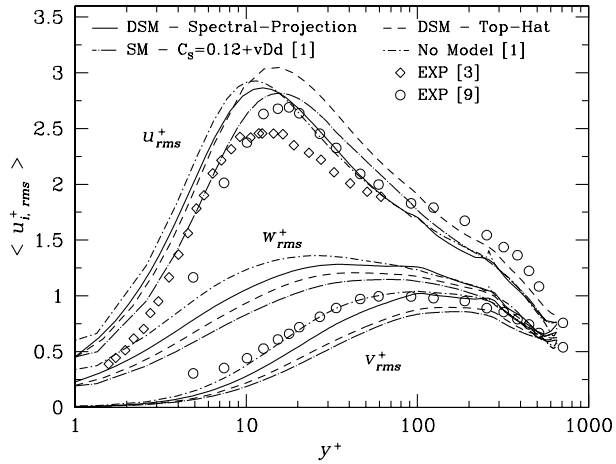

Figure 4: Mean rms-values of the velocity fluctuation.

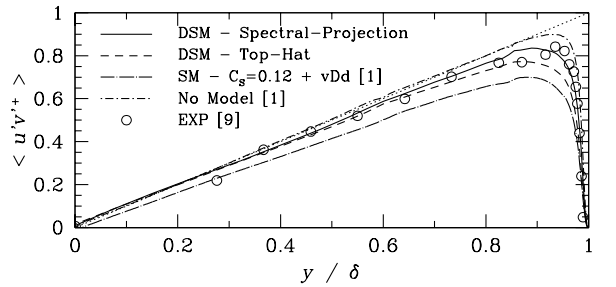

Figure 5: Mean shear-stress profiles.

figure 5, all profiles approach the linear distribution of the total shear stress, indicated by the dotted line. The Smagorinsky model predicts the lowest level of resolved shear-stress, while the dynamic models give marginally larger values, besides a slight difference of both dynamic solutions.

For comparison with the fixed-constant Smagorinsky model, the value C_S can be reconstructed from the time-averaged mixing-length profiles using the same mesh size $\overline{\Delta}$ as employed in the Smagorinsky model. As can be seen from figure 6, the spectral-projection filter gives a significantly lower value than the top-hat filter. The fact that the tailored Smagorinsky model with $C_S = 0.12$ and the dynamic model with the spectral-projection filter give the best results, confirms that the correct level of C_S should be in the range of $0.06 - 0.12$. Both filters used in the dynamic procedure correctly switch off the model at the wall, as expected. Due to the local nature of the model, the dynamic estimate varies in each element, while giving an overall symmetric distribution over the channel. Apparently, negative values of the model constant do not persist in the time-average, although negative values do occur during the simulation.

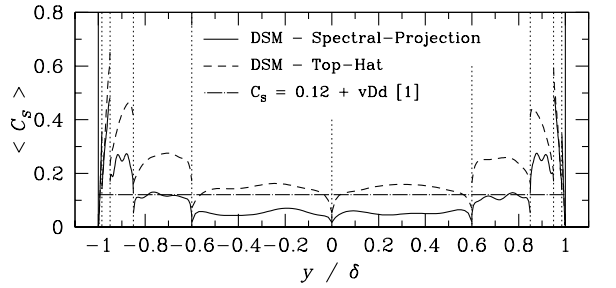

Figure 6: Profiles of the dynamic model parameter C_S.

Conclusions

The dynamic Smagorinsky model has been implemented into a spectral element method and successfully applied to simulation of a turbulent channel flow. The results give good agreement with reference data and are obviously affected by the test filter function applied within the dynamic procedure. The reason for the differences in the dynamic model solutions might be caused by the fixed length-scale ratio $(\widetilde{\overline{\Delta}}/\overline{\Delta}) = 2$, which is used by both filters, although they obviously act differently on the resolved flow field. The dynamic procedure implicitly gives zero model values at the wall as required and the general implementation retains the applicability of the method to complex geometry turbulent flows.

Acknowledgements

The support of the Australian Partnership for Advanced Computing (APAC) is gratefully acknowledged.

References

[1] Blackburn, H. M., Channel Flow LES with Spectral Elements, in *13th Australasian Fluid Mechanics Conference*, Monash University, 1998, 989–992, 989–992.

[2] Germano, M., Piomelli, U., Moin, P. and Cabot, W. H., A dynamic subgrid-scale eddy viscosity model, *Physics of Fluids*, **A3**, 1991, 1760–1765.

[3] Hussain, A. K. M. F. and Reynolds, W. C., Measurements in Fully-Developed Turbulent Channel Flow, *ASME J. Fluid Engng*, **97**, 1975, 568–578.

[4] Karniadakis, G. E. and Henderson, R. D., Spectral Element Methods for Incompressible Flows, in *Handbook of Fluid Dynamics*, editor R. W. Johnson, CRC Press, Boca Raton, 1998, 29–1–29–41.

[5] Karniadakis, G. E., Orszag, S. A. and Yakhot, V., Renormalization Group Theory Simulation of Transitional and Turbulent Flow over a Backward-Facing Step, in *Large Eddy Simulation of Complex Engineering and Geophysical Flows*, editors B. Galperin and S. A. Orszag, Cambridge, 1993, 159–177.

[6] Karniadakis, G. E. and Sherwin, S. J., *Spectral/hp Element Methods for CFD*, Oxford University Press, 1999.

[7] Levin, J. G., Iskandarani, M. and Haidvogel, D. B., A Spectral Filtering Procedure for Eddy-Resolving Simulations with a Spectral Element Ocean Model, *J. Comput. Phys.*, **137**, 1997, 130–154.

[8] Lilly, D., A proposed modification of the Germano subgrid-scale closure method, *Physics of Fluids*, **A4**, 1992, 633–635.

[9] Wei, T. and Willmarth, W., The Reynolds number effect on the small scale structure of a turbulent channel flow, *JFM*, **204**, 1989, 57–95.

[10] Zang, T. A., On the Rotation and Skew-Symmetric Forms for Incompressible Flow Simulations, *Appl. Num. Math.*, **7**, 1991, 27–40.